ISSN 0026-8933, Molecular Biology, 2024, Vol. 58, No. 5, pp. 944–960. © Pleiades Publishing, Ltd., 2024.

CELL MOLECULAR BIOLOGY

UDC 575:599.9

Expression of Long Noncoding RNAs and Protein-Coding Genes Involved in Oxidative Stress and Cell Senescence in Patients with Chronic Obstructive Pulmonary Disease

V. A. Markelov[a, b], G. F. Korytina[a, b, *], Y. G. Aznabaeva[b], I. A. Gibadullin[b], L. Z. Akhmadishina[a, c], T. R. Nasibullin[a], O. V. Kochetova[a], A. M. Avzaletdinov[b], and N. Sh. Zagidullin[b]

[a] *Institute of Biochemistry and Genetics—Subdivision of the Ufa Federal Research Centre of the Russian Academy of Sciences, Ufa, 450054 Russia*

[b] *Bashkir State Medical University, Ufa, 450008 Russia*

[c] *Ufa State Petroleum Technological University, Ufa, 450064 Russia*

**e-mail: guly_kory@mail.ru*

Received January 23, 2024; revised April 10, 2024; accepted April 22, 2024

Abstract—Chronic obstructive pulmonary disease (COPD) is a multifactorial heterogeneous chronic inflammatory respiratory disease. The molecular pathogenesis of COPD may include dysregulation of the stress responses that are associated with cell senescence and involve a wide range of signaling pathways and their epigenetic regulators, such as long noncoding RNAs (lncRNAs). To assess the contribution of genes involved in key signaling pathways related to cell senescence to the molecular pathogenesis of COPD, expression profiling of lncRNA (*TP53TG1*, *LINC00342*, *H19*, *MALAT1*, *DNM3OS*, and *MEG3*) and protein-coding (*PTEN*, *TGFB2*, *FOXO3*, and *KEAP1*) genes was performed in peripheral blood mononuclear cells of COPD patients ($n = 92$) and control subjects ($n = 81$). Significant downregulation of the *TP53TG1* and *DNM3OS* lncRNAs and the *TGFB2* mRNA was observed in the COPD patients, while the *MALAT1* and *LINC00342* were upregulated. A highly informative prognostic model was constructed based on the multiple regression and ROC analyses. The model included simultaneous assessment of the *TP53TG1* and *TGFB2* expression levels (AUC = 0.92). *MALAT1*, *DNM3OS*, *TGFB2*, *FOXO3* and *KEAP1* expression levels were found to positively correlate with lung function parameters, reflecting the disease progression. The lncRNA (*TP53TG1*, *LINC00342*, *DNM3OS*, and *MALAT1*) and protein-coding (*TGFB2*) genes that were differentially expressed in the COPD patients are functionally involved in regulating apoptosis, inflammation, fibrogenesis, and the epithelial-to-mesenchymal transition, implicating cell senescence processes in the molecular pathogenesis of COPD.

Keywords: chronic obstructive pulmonary disease, oxidative stress, cell senescence, long noncoding RNAs

DOI: 10.1134/S0026893324700481

INTRODUCTION

Chronic obstructive pulmonary disease (COPD) is a multifactorial heterogeneous chronic inflammatory disease that affects distal airways (bronchi and bronchioles) and lung parenchyma and leads to pulmonary emphysema [1]. Along with cardiovascular disorders and cancer, COPD is a major cause of deaths in the global population, and new approaches to its diagnosis and treatment are sought continuously [2]. COPD results from complex interactions of molecular genetic factors, a network of epigenetic regulators, and environmental factors tightly associated with lifestyle [3].

Inhalation of tobacco smoke particles and other pollutants and activation of inflammatory cells (macrophages and neutrophils) lead to oxidative stress [2, 3], which is thought to play a crucial role in accelerated cell senescence because reactive oxygen species damage cell structures [4].

Evidence is accumulating to associate COPD with accelerated aging and excess accumulation of senescent cells with an irreversible arrest of the cell cycle [5]. COPD is characterized by telomere damage and shortening [6], DNA damage [7], a substantially lower regenerative potential of basal and type II alveolar epithelial cells [8], and an accumulation of cells expressing a senescence-associated secretory phenotype (SASP) [7].

Mechanisms associated with the function of long noncoding RNAs (lncRNAs) are of particular interest because lncRNAs play an important role in regulating various intracellular signaling pathways and producing various pathological phenotypes [9]. Nuclear lncRNAs are involved in compartmentalization of the

nucleus, splicing regulation, and gene activity and perform their functions by interacting allosterically with transcription factors and maintaining the euchromatin structure and heterochromatin formation [10]. Cytoplasmic lncRNAs bind with microRNAs to prevent their inhibitory effect on mRNAs (i.e., they act as competitive endogenous RNAs (ceRNAs)), regulate structural modifications of proteins, provide a scaffold for proteins involved in signaling cascades, and play a role in the formation of intercellular junctions [11].

We have previously described the role that lncRNAs and cell senescence play in the COPD pathogenesis [12]. In this work, expression profiling of several lncRNAs and protein-coding genes involved in regulating cell senescence was carried out in COPD patients. The *TP53TG1* (TP53 target 1) codes for a lncRNA of the same name, is induced by the p53 tumor suppressor protein, is in chromosome 7q21, is involved in the cell response to damage, and acts as a component of the TP53 signaling pathway [13]. The TP53TG1 lncRNA inhibits WNT/β-catenin and promotes cell apoptosis by activating synthesis of PTEN and inhibiting the PI3K/AKT signaling pathway [13, 14], which is associated with various processes, such as cell proliferation, adhesion, migration, invasion, metabolism, survival, and aging [15]. The *LINC00342* (long intergenic non-protein coding RNA 342) gene is in chromosome 2 (2q11.1) and codes for a lncRNA of the same name; its expression is upregulated in non-small cell lung cancer tissues [16]. The LINC00342 lncRNA binds with miR-203a-3p [17], thus suppressing antitumor activities of p53 and PTEN [18]. *DNM3OS* (dynamin 3 opposite strand/antisense RNA) is in chromosome 1q24.3, is transcribed to produce a lncRNA, and includes three microRNA sequences: miR-199a-5p, miR-199a-3p, and miR-214-3 [19]. DNM3OS acts as a fibroblast-specific effector in TGF-β-induced pulmonary fibrosis [20]. The *MALAT1* (metastasis-associated lung adenocarcinoma transcript 1) gene is in chromosome 11q13.1 and is involved in regulating the cell response to oxidative stress and the processes of cell senescence [21]. MALAT1 inhibits *TP53* expression at the pre-mRNA level; increases expression of *MMP9* and *PIK3CA*; and activates the PI3K/AKT signaling cascade, which is associated with cell senescence [21]. The *H19* (imprinted maternally expressed transcript) gene is in chromosome 11p15.5. The H19 lncRNA acts as a key component of regulatory networks involved in the pathogenesis of certain cancers [22] and fibrosis. Its effect is mediated by stimulation of autophagy, inhibition of apoptosis, an increase in the epithelial-to-mesenchymal transition (EMT), and activation of the TGF-β/SMAD3 and mTOR signaling pathways [23, 24]. The *MEG3* (maternally expressed 3) gene is in region 14q32.2. The MEG3 lncRNA regulates the mitochondrial pathway of apoptosis by activating p53 and inhibiting Bcl-xl [25]. MEG3 overexpression decreases the TGF-β1 level, activity of the PI3K/AKT pathway, and EMT [26]. The *PTEN* (phosphatase and tensin homolog) gene is in chromosome 10q23 and codes for a protein that acts as a functional antagonist of the PI3K/AKT/m-TOR signaling pathway [27] and plays an important role in glycolysis, glycogen synthesis, lipid metabolism, and mitochondrial metabolism [28]. The *TGFB2* gene is in chromosome 1q41. Its protein product belongs to the TGF-β family and regulates cell proliferation, differentiation, migration, regeneration, and apoptosis; intercellular matrix remodeling; and EMT induction [29]. Cytokines of the TGF-β family act as ligands of the TGFBRI, TGFBRII, and TGFBRIII receptors and activate the canonical TGF-β/SMAD2/SMAD3/SMAD4 pathway [30]. *FOXO3* is in chromosome 6q21 and codes for a protein belonging to the FOX transcription factor family (FOXO subfamily) [31]. FOXO3 is controlled predominantly by the PI3K/AKT signaling pathway. An active dephosphorylated form of FOXO3 is associated with the control of protein metabolism, autophagy, and cell apoptosis [30]. The *KEAP1* (kelch-like ECH-associated protein 1) gene is in chromosome 19p13.2 and codes for an endogenous inhibitor of Nrf2 (NFE2-like bZIP transcription factor 2). The KEAP1–NRF2 complex regulates oxidative homeostasis and cell senescence and survival [32].

To estimate the contribution to the molecular pathogenesis of COPD for genes whose products are components of key signaling cascades associated with oxidative stress and cell senescence, the expression profile of lncRNAs (TP53TG1, LINC00342, H19, MALAT1, DNM3OS, and MEG3) and protein-coding genes (*PTEN*, *TGFB2*, *FOXO3*, and *KEAP1*) was studied in peripheral blood mononuclear cells (PBMCs) of COPD patients.

EXPERIMENTAL

All studies were conducted in accordance with good clinical practice regulations and the principles of biomedical ethics as outlined in the 1964 Declaration of Helsinki and its later amendments. They were also approved by the Ethics Committee of the Institute of Biochemistry and Genetics (Ufa), protocol no. 19 dated November 1, 2022. Each participant in the study provided a voluntary written informed consent for providing biological material. The study was a case–control study and compared COPD patients (n = 92) and control subjects (n = 81). The COPD patients received in-patient treatment at the Pulmonology Department of City Clinical Hospital no. 21 or the Thoracic Department of the Clinics of Bashkir State Medical University (Ufa). COPD was diagnosed according to the recommendations of the Global Strategy for the Diagnosis, Management, and Prevention of Chronic Obstructive Lung Disease (http://goldcopid.org) and was based on clinical, laboratory, and instrumental tests, including high-resolution computed tomography and spirometry.

Table 1. Characteristics of the subject groups

Parameter	COPD ($n = 92$)	Control ($n = 81$)	P
Age (mean ± SD)	58.49 ± 15.46	54.46 ± 14.43	0.27
Women (n, %)	4 (4.35)	6 (7.41)	0.259
Men (n, %)	88 (95.65)	75 (92.59)	
Nonsmokers (n, %)	12 (13.04)	11 (13.58)	0.891
Smokers (n, %)	80 (86.96)	70 (86.42)	
Smoking index, pack-years (mean ± SD)	39.37 ± 18.63	20.5 ± 15.1	0.0089
BMI (mean ± SD)	25.48 ± 5.27	25.77 ± 4.31	0.702
FEV1/FVC, % (mean ± SD)	61.64 ± 25.8	98.07 ± 22.26	0.0001
VC, % (mean ± SD)	57.94 ± 15.4	92.9 ± 21.83	0.5572
FVC (mean ± SD)	45.01 ± 18.22	106.32 ± 31.14	0.0001
FEV1, % (mean ± SD)	55.72 ± 23.63	69.78 ± 24.09	0.022

BMI, body mass index; VC, vital capacity; FVC, forced vital capacity; FEV1, forced expiratory volume in the first second. Smoking index was calculated as the number of cigarettes smoked per day × number of years the subject has smoked/20.

All patients received dual bronchodilator therapy, including a long-acting β2 agonist in combination with a long-acting cholinergic antagonist, in accordance with the Federal Clinical Recommendations for COPD Diagnosis and Treatment [1].

A control group included unrelated subjects who had no history of chronic diseases, including respiratory disorders, and no signs of acute respiratory disease at the time of material collection. All subjects underwent clinical and instrumental testing, including measurements of the body mass index (BMI) and the breathing parameters: vital capacity (VC), forced vital capacity (FVC), forced expiratory volume in the first second (FEV1), and FEV1/FVC ratio. The proportion of smokers was determined, and the smoking index calculated. The inclusion criteria for the control group included normal values of the breathing parameters (FEV1/FVC > 70% and FEV1 > 80%) and an age >45 years. Clinical and demographic characteristics of the groups are summarized in Table 1.

Analysis of lncRNA, microRNA, and mRNA interactions. The genome databases KEGG (Kyoto Encyclopedia of Genes and Genomes, https://www.k egg.jp/), TarBase v. 8.0 (https://dianalab.e-ce-uth.gr/html/diana/web/index.php?r=tarbasev8), and miRTarBase v. 8.0 (https://mirtarbase.cuhk. edu.cn/~miRTarBase/miRTarBase_2019/php/download. php) were used to perform a preliminary in silico analysis and to identify the interacting mRNAs, microRNAs, and lncRNAs that are involved in key signaling cascades associated with oxidative stress and cell senescence. The online tools NetworkAnalyst 3.0 (https://www.networkanalyst.ca/NetworkAnalyst/) and Lncrna2target v. 3.0 (http://bio-annotation.cn/lncrna2target/browse.jsp, accessed August 17–23, 2023) [33] were used to interpret the gene list and to identify pairwise interactions in the network. Files that contained parameters of the nodes and edges of the network were modified to include the additional data obtained by analyzing the gene list in the NCBI PubMed database (https://pubmed. ncbi.nlm.nih.gov). The resulting attributive dataset obtained for the gene network was used to visualize the interactions of lncRNAs, microRNAs, and mRNAs with the help of Cytoscape v. 3.10.0.

RNA isolation from PBMCs. Peripheral blood monocytes and lymphocytes play an active role in the pathogenesis of COPD and are involved in maintaining and controlling the inflammatory process in COPD. PBMCs were therefore used to assess the lncRNA and mRNA expression levels. Specifics of the expression profile of regulatory noncoding RNAs and protein-coding genes in MNCs of COPD patients may provide noninvasive biomarkers of the disease.

Peripheral blood samples (4 mL) were collected in K3 EDTA vacuum tubes and transferred into the laboratory within 1 h of collection. PBMCs were isolated by a standard method of density gradient centrifugation with 3 mL of Ficoll-Paque GE (Cytiva, density 1.077 g/mL). A blood sample (4 mL) was diluted with an equal volume of Dulbecco's phosphate-buffered saline (DPBS, without Ca and Mg, BioloT, Russia) and layered on top of 3 mL of Ficoll-Paque. The tube was centrifuged at 420 *g* at room temperature for 30 min. MNCs at the interphase were collected, washed twice with DPBS to remove Ficoll-Paque and plasma traces, transferred into another tube, and combined with 1 mL of TRIzol Reagent (Thermo Fisher Scientific, United States) for RNA isolation. Total RNA of PBMCs was isolated using TRIzol (Invitrogen, United States), www.invitrogen.com) as recommended by the manufacturer. The mRNA amount (ng/μL) and quality were assessed by measuring absorption at 260 nm with a NanoDrop 1000 spectro-

Table 2. Genes, primers, and probes used in this work

Gene (ID)*	Locus	Primer and probe nucleotide sequences (5' → 3')
TP53TG1 (ID: 11257)	7q21.12	TP53TG1-F: GGCTCTTTCCTTTAATCTTCGG TP53TG1-R: GAATTGTTACCAGGGTTACTCAGAC TP53TG1-Probe: FAM-TGCCCAACTCAGGTTTAACCACCA-BHQ1
LINC00342 (ID: 150759)	2q11.1	LINC00342-F: TTTCATCTGAAGCAGCAGAGTG LINC00342-R: CAGTTGTGGTGATCTTTGTTCCTG LINC00342-Probe: FAM-CAGAGTCAGGTCACCAACCAGTGTGGA-BHQ1
H19 (ID: 283120)	11p15.5	H19-F: GAATCGGCTCTGGAAGGTGA H19-R: GCTGCTGTTCCGATGGTG H19-Probe: FAM-CCAGACCTCATCAGCCCAACATC-BHQ1
MALAT1 (ID: 378938)	11q13.1	MALAT1-F: GAACACAAGAAGTGCTTTAAGAGGC MALAT1-R: GCGAGGCGTATTTATAGACGG MALAT1-Probe: FAM-AGGTGATCGAATTCCGGTGATGC-BHQ1
DNM3OS (ID:100628315)	1q24.3	DNM3OS-F: GGGACACTGCTGAGAAAAGACTG DNM3OS-R: GCTCACTGTTGGTTAGTTTCCTC DNM3OS-Probe: FAM-ATCCCCGCTGGTCTTCCCTTCG-BHQ1
MEG3 (ID: 55384)	14q32.2	MEG3-F: GCCCATCTACACCTCACGAG MEG3-R: CCTCTTCATCCTTTGCCATCC MEG3-Probe: FAM-CCCACCAACATACAAAGCAGCCACT-BHQ1
PTEN (ID: 5728)	10q23.31	PTEN-F: CACACGACGGGAAGACAAGT PTEN-R: CCTCTGGTCCTGGTATGAAGAA PTEN-Probe: FAM-CCCTCAGCCGTTACCTGTGTGTG-BHQ1
TGFB2 (ID: 7042)	1q41	TGFB2-F: TGCCGCCCTTCTTCCC TGFB2-R: CATTCTTCTCCATTGCTGAGAC TGFB2-Probe: FAM-CCATCCCGCCCACTTTCTACAGAC-BHQ1
FOXO3 (ID: 2309)	6q21	FOXO3-F: GGGAAGTGGGCAAAGCAGA FOXO3-R: GCGTGGGATTCACAAAGG FOXO3-Probe: FAM-ACCCTTTGCCAAATCTGCTCTC-BHQ1
KEAP1 (ID: 9817)	19p13.2	KEAP1-F: CAACAGTGTGGAGAGGTATGAGC KEAP1-R: AAGGAGACGATTGAGGACAGC KEAP1-Probe: FAM-CCCCAATGCTGACACGAAGGATC-BHQ1

*Gene IDs are as in the database at https://www.ncbi.nlm.nih.gov/gene.

photometer (Thermo Fisher Scientific). RNA quality was inferred from the A_{260}/A_{280} ratio, which is expected to range 1.8–2.0. Phenol ring-containing components were similarly detected by A_{260}/A_{230}. RNA integrity was assessed by electrophoresis in 1% agarose gel with 0.5 μg/mL ethidium bromide, using the 28S and 18S rRNA bands. To remove DNA, all RNA samples were digested with RNase-free DNase I (Thermo Fisher Scientific).

Synthesis of cDNA and analysis of lncRNA and mRNA expression. The first cDNA strand was synthesized using random hexamer primers and a First Strand cDNA Synthesis kit for RT-qPCR (Thermo Fisher Scientific) as recommended by the manufacturer. RNA samples were standardized by bringing the RNA concentration to 100 ng/μL to synthesize cDNA. The reaction mixture (20 μL) contained 3 μL of template RNA, 1 μL of random primers, 4 μL of a 5× reaction buffer (250 mM Tris-HCl, pH 8.3, 250 mM KCl, 20 mM $MgCl_2$, 50 mM DTT), 1 μL of RiboLock RNase inhibitor (20 units/μL), 2 μL of 10 mM dNTP mixture, 1 μL of RevertAid M-MuLV reverse transcriptase (200 units/μL), and nuclease-free water to 20 μL. The mixture was incubated at 25°C for 5 min, 42°C for 60 min, and 70°C for 5 min. The reverse transcription product was stored at –70°C until used for quantitative PCR. Quantitative PCR was carried out in a 96-well plate, using a qPCRmix-

Table 3. Functional characteristics of the lncRNAs and mRNAs examined in this work

Gene	Target	Function
TP53TG1	miR-18a-5p, ACTA2, FN1	Proapoptotic effect on lung cells, antifibrotic effect
LINC00342	miR-15b/TPBG, miR-15b/BCL2, miR-203a-3p/SIX1	EMT regulation, stimulation of inflammatory process in the lung
H19	miR-29b, miR-29a-3p, miR-196a, miR-140, miR-21/PTEN/AKT, miR-122-5p, miR-675-3p/IGF1R, miR-200a, miR-19b-3p/FTH1, miR-130a-3p/WNK3, miR-193a-3p, miR-138	Profibrotic effect, stimulation of inflammatory process in the lung, proapoptotic effect, increase in EMT
MALAT1	miR-101-3p/MCL1, miR-101/SOX9 (Wnt pathway), miR-200a-3p, miR-200b-3p, miR-200c-3p, miR-206 (Akt/mTOR pathway), miR-202-3p/RRM2, miR-202-3p/CCND1, miR-129-5p/YWHAB, miR-129-5p/MCRS1, miR-129-5p/CDH1, miR-129-5p/VIM, miR-129-5p/HMGB1 miR-374b-5p/SRSF7, miR-374b-5p/ FOXP1 miR-613, miR-613/COMMD8, miR-613/GJA1, miR-613/CDK4, miR-19b-3p/PPP2R5E, miR-19b-3p/BCL2L11, miR-17-5p/FOXA, miR-1297/TRIB2, miR-375/YAP, miR-194-5p/FOXP2, miR-194-5p/FOXK1, miR-503-5p, miR-590, miR-590/YAP1, miR-150/eIF4E/Akt, miR-22-3p/NLRP3, miR-375, miR-23c, miR-429	Antiapoptotic effect, profibrotic effect, increase in EMT, stimulation of inflammatory process in the lung, emphysema-promoting effect
DNM3OS	Predecessor miR199a-5p/3p, miR-214-3p; miR-204-5p/AP1S2, miR-199a-5p/3p/SIRT1, miR-181a-5p/STAT3	Profibrotic effect
MEG3	miR-181a-5p/Bcl-2, miR-181a-5p/PTEN, miR-181d-5p/CDKN3, miR-181a-5p/PTEN/pSTAT5/SOCS1, miR-181b-5p/JAK2/STAT3, miR-181b-3p, miR-140-5p*/TLR4, miR-140-5p/MMD, miR-140-5p/YES1, miR-140-5p (Wnt pathway) miR-125a-5p, miR-125a-5p/STAT3, miR-125a-5p/Sp1/SIRT1/HIF-1α, MDM2, TP53, TP63, KRT14, STAT3, YAP1, TP73, SOX2, HES1, HEY1 AXL, MDM2, JARID2, EZH2; miR-133a-3p/ IGF1R TGF-β/Smad3 pathway), miR-133a-3p/SIRT1, miR-770-5p/TGFBR1, miR-664a-3p/FHL1	Antiapoptotic effect, increase in EMT, stimulation of inflammatory process in the lung, emphysema-promoting effect, stimulation of cell aging
TGFB2	miR-454-3p, miR-193a-3p	Increase in EMT, antiapoptotic effect
PTEN	miR-19b-3p, miR-23a-3p, miR-217-5p, miR-221-3p, miR-222-3p, miR-486-5p, miR-425-5p, miR-18a-5p, miR-543, miR-20b-5p, miR-21, miR-216a, miR-181a-5p	Antiapoptotic effect, profibrotic effect, EMT regulation
FOXO3	miR-182, miR-217, miR-29b-3p, miR-23a	Antiapoptotic effect, proapoptotic effect
KEAP1	miR-421 miR-432-3p, MALAT1, miR-125b-5p, miR-141-3p	Antiapoptotic effect, regulation of antioxidant cell defense

Interactions of lncRNAs and microRNAs with mRNAs were analyzed using the online tool NetworkAnalyst 3.0 (https://www.networkanalyst.ca/NetworkAnalyst/) and the integrated databases KEGG, miRTarBase v. 8.0, and TarBase v. 8.0; the online tool Lncrna2target v. 3.0 (http://bio-annotation.cn/lncrna2target/browse.jsp); and NCBI PubMed (https://pubmed.ncbi.nlm.nih.gov/).

HS Master Mix (Evrogen, Russia, https://evrogen.ru) and a QuantStudio 5 system (Applied Biosystems, United States). The following lncRNA and protein-coding genes were selected for the analysis based on the results of a bioinformatics search: *TP53TG1*, *LINC00342*, *H19*, *MALAT1*, *DNM3OS*, *MEG3*, *PTEN*, *TGFB2*, *FOXO3*, and *KEAP1*. Target gene expression levels were estimated using sets of gene-specific primers (10 ng/μL) and fluorescent probes (10 ng/μL), which were designed and synthesized by DNA-Sintez (Russia). Characteristics of the selected genes are summarized in Table 2. The *B2M* housekeeping gene (ID567) was used as an internal control. The B2M mRNA level was assessed using the gene-specific primers and probe (Hs00187842m1, Thermo Fisher Scientific). RT-PCR was run in triplicate for each sample and included initial denaturation at 95°C for 3 min and 45 cycles of denaturation at 95°C for 15 s and amplification at 60°C for 1 min. Quality was checked using a positive control, which was provided by the kit manufacturer, and a negative control, which did not contain cDNA.

Statistical analyses were carried out using GraphPad Prism 9 software (GraphPad Software, https://www.graphpad.com) and IBM SPSS Statistics 22.0. The mean and standard deviation (mean ± SD) and the median and 25–75% interquartile range (median, 25–75% IQR). Groups were compared using the nonparametric Mann–Whitney U test (when the data distribution was other than normal) or Student's *t*-test (when the data were distributed normally). Qualitative character frequencies were compared by the χ^2 test. Results were considered significant at $P < 0.05$. Relative expression levels were assessed by the $\Delta\Delta C$t method, which is based on the assumption that the difference in threshold cycle (ΔCt) between a target and a reference gene is proportional to the relative expression level of the target gene. Results were normalized to the expression level of the *B2M* housekeeping gene as follows: $\Delta C\text{t} = C\text{t}$ (target gene) $- C$t (housekeeping gene) [34]. Relative expression levels were represented as $2^{-\Delta\Delta Ct}$ [34]. Differences in relative expression level between the patients and controls were evaluated using the nonparametric Mann–Whitney U test. Fold Change (FCh) in expression in the COPD patients was assessed as compared with the controls ($2^{(-\Delta\Delta Ct)}$ COPD/$2^{(-\Delta\Delta Ct)}$ control), and a fold decrease or a fold increase in expression (Fold Regulation (FR)) was calculated for the patients. In the case of FCh < 1, FR = −1/FCh. A correlation between variables was assessed via a nonparametric analysis with Spearman's coefficient of correlation. Prognostic significance was evaluated via a receiver operating characteristic (ROC) analysis with calculations of the area under the curve (AUC), sensitivity, and specificity. The most significant models were identified by a multiple regression analysis with stepwise inclusion of significant predictors; a ROC analysis was then performed to estimate the efficiency of a prognostic model.

RESULTS

Analysis of mRNA, microRNA, and lncRNA Interaction Network

A preliminary *in silico* analysis was carried out to identify the network of interacting mRNAs, microRNAs, and lncRNAs. Functional characteristics of the lncRNAs and mRNAs selected for the study are summarized in Table 3. A visualization of the network of interacting noncoding RNAs (lncRNAs and microRNAs) and mRNAs is shown in Fig. S1 (see Supplementary Information at http://www.molecbio.ru/downloads/2024/5/supp_Markelov_rus.zip).

Several prognostic online tools were employed in our *in silico* analysis. Parameters of binding sites of coregulated RNAs and, in particular, their binding energy are of particular importance in this context. Binding energy is assumed to depend on the size of a binding site [35]. Noncoding RNAs bind preferentially with high-affinity sequences of 7 or 8 nt and slightly weaker with 6-nt sequences [36–38]. According to the assumption, high affinity was expected for the majority of binding sites predicted in our *in silico* analysis. The abundance of individual target genes is capable of modulating activity of noncoding RNAs. A sensitivity threshold is therefore possible for the concentrations of an effector noncoding RNA and its target transcripts [35]. To efficiently interact with a noncoding RNA, target transcripts must be expressed to an extremely high levels, which exceed their physiologically normal expression levels [39].

Functional characteristics of the TP53TG1 lncRNA network is limited to proapoptotic and antifibrotic potentials [40, 41].

Targeted interactions of the LINC00342 lncRNA are associated with an increase in EMT and inflammatory processes [42–44].

The functional interaction network of the H19 lncRNA includes proapoptotic and profibrotic axes and is associated with an increase in inflammation in lung tissue and higher EMT [22, 23, 45]. The MALAT1 lncRNA is associated mostly with EMT. For example, the interactions of MALAT1 with certain microRNAs increase EMT and activate the AKT/mTOR signaling cascade [46–49]. MALAT1 exerts profibrotic and emphysema-promoting effects [50] and increases inflammatory processes in the lung [21] (Table 3).

The MEG3 lncRNA activates the TGF-β/SMAD3 [51] and Wnt signaling cascades and plays a role in EMT regulation [52]. MEG3 acts to regulate apoptosis in lung cells, and its binding with miR-181a activates BCL2 [53]. Several molecules included in the MEG3 interaction network play important roles in COPD pathogenesis. MEG3 can inhibit the miR-

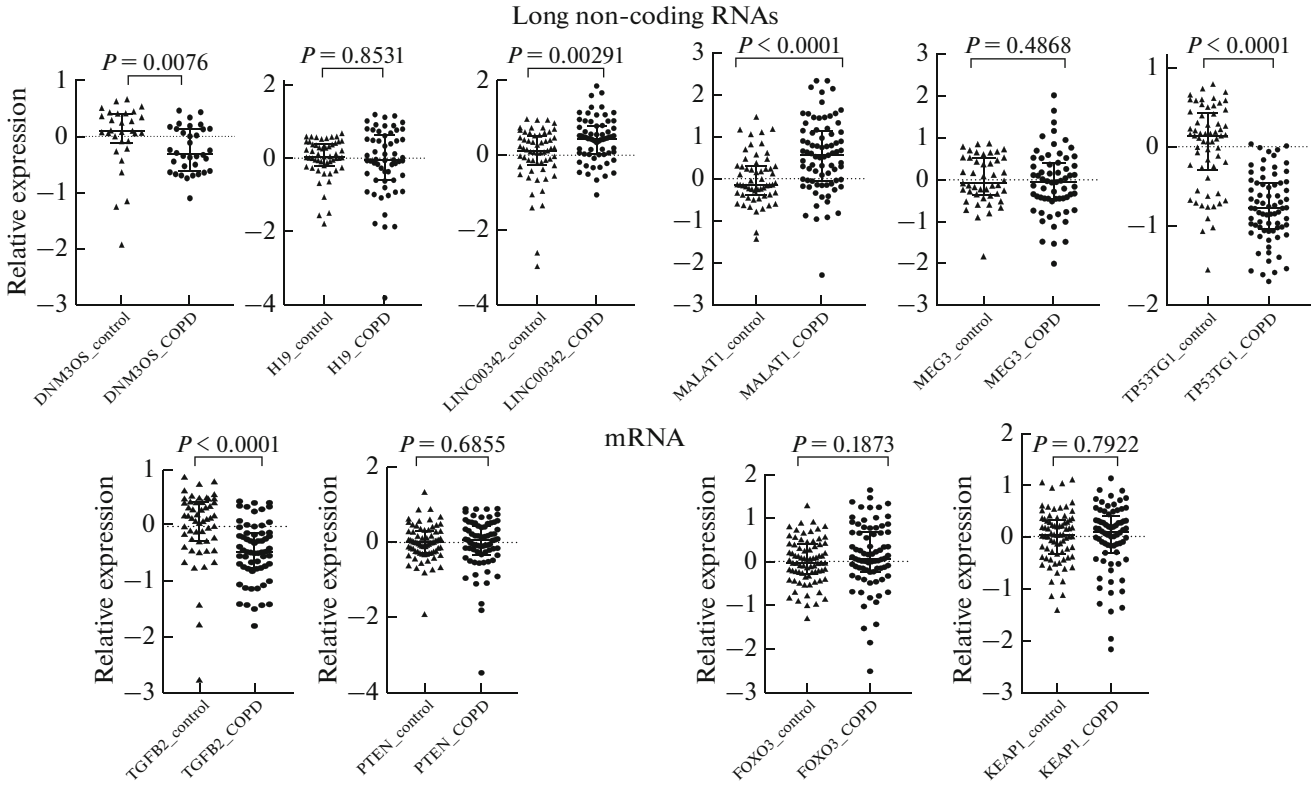

Fig. 1. Relative expression (presented as log10 of Fold Change ($\log10\ 2^{-\Delta\Delta Ct}$) of the lncRNAs and mRNAs in the COPD patients and control subjects. Results are shown as the median and 25–75% interquartile range (IQR); *P* is the significance level by the Mann–Whitney U test.

181a-5p function and thus cause subsequent stimulation of the PTEN/pSTAT5/SOCS1 signaling cascade in macrophages in acute respiratory distress syndrome [54]. A similar mechanism underlies the interaction of MEG3 with miR-181b-5p, which modulates the JAK2/STAT3 signaling cascade and thereby regulates macrophage polarization to a M2-like phenotype. MEG3 is potentially capable of preventing this effect to stimulate the proinflammatory phenotype of macrophages [55]. The emphysema-promoting axis includes a single target molecule, miR-181b-3p, which is associated with pathological angiogenesis and, therefore, emphysema initiation in the lung [50]. By binding with miR-125a-5p and thus regulating the Sp1/SIRT1/HIF-1α signaling cascade, MEG3 is capable of delaying senescence in lung epithelial cells [56].

The DNM3OS lncRNA interacts with molecules associated with profibrotic and proinflammatory effects. For example, DNM3OS is involved in regulating the TGF-β-induced activation of lung myofibroblasts [20]. According to our in silico analysis, miR-181a-5p is a target of DNM3OS. In turn, the anti-inflammatory effect of miR-181a-5p is related to its potential to regulate the PTEN-pSTAT5-SOCS1 signaling cascade [54].

Protein-coding genes were also included in the list of genes selected for the study. A protein–protein interaction network of the products of the selected genes is shown in Fig. 2S (see Supplementary Information at http://www.molecbio.ru/downloads/2024/5/supp_Markelov_rus.zip). The network includes three large clusters of protein–protein interactions involving KEAP1, PTEN, and FOXO3 and a minor cluster based on TGF-β2.

Interactions of *PTEN* with microRNAs (miR-19b-3p, miR-23a-3p, miR-486-5p, etc.) decrease the PTEN level by activating the PI3K/AKT signaling cascade and decreases cell apoptosis [57]. Binding with *PTEN*, miR-181a-5p stimulates EMT in lung adenocarcinoma cells [58]. A fibrosis-related functional network includes two microRNAs, miR-21 and miR-216a, which bind with *PTEN* to modulate proliferation and migration of airway smooth muscle cells, which subsequently undergo hyperplasia and become capable of acquiring the EMT phenotype [45]. In the context of emphysema-like changes that arise in airways in COPD, the interaction of PTEN with the N-terminal domain of the serum response factor (SRF) is of particular interest, stimulating transcriptional activity of SRF and normal proliferation of vascular smooth cells [59].

Table 4. Relative expression levels of the genes under study in the COPD patients

Gene	Fold change	Fold regulation	*P*
TP53TG1	0.1532	−6.5244	0.0001
LINC00342	2.874	2.874	0.0029
MALAT1	6.983	6.983	0.0001
H19	1.764	1.764	0.8531
DNM3OS	0.5176	−1.9317	0.0076
MEG3	2.304	2.304	0.4868
PTEN	1.087	1.087	0.6855
TGFB2	0.3639	−2.7476	0.0001
FOXO3	2.246	2.246	0.1873
KEAP1	1.0513	1.0513	0.7922

Fold change = $2^{(-\Delta\Delta Ct)}$ COPD/$2^{(-\Delta\Delta Ct)}$ control. In the case of Fold change < 1, Fold regulation = −1/Fold change. *P* is the significance level by the Mann–Whitney U test.

Table 5. Predictive regression model of COPD development

Predictor	Coefficient β	P_{Wald}	*OR*	95% CI
Relative expression of *TGFB2*	0.898	0.004	2.456	1.33–4.54
Relative expression of TP53TG1	3.365	6.9×10^{-5}	28.939	5.52–151.8
Regression constant	−3.032	0.000	0.048	
$P = 6.02 \times 10^{-12}$, AUC = 0.92 (95% CI 0.86–0.98), sensitivity 73.2%, specificity 92.3%				

P_{Wald}, significance by the Wald test; *OR* = exp(β), odds ratio; *P*, value in the likelihood-ratio test; AUC, area under the curve; 95% CI, asymptotic 95% confidence interval of AUC. The ROC curve is shown in Fig. 2.

A network of target molecules of the *FOXO3* protein-coding genes is related to apoptosis. For example, *FOXO3* binding with miR-182 promotes resistance to radiotherapy-induced apoptosis in non-small cell lung cancer cells [60]. In contrast, *FOXO3* binding with miR-23a decreases the proliferative potential and delays the cell cycle in lung fibroblasts [61]. The interaction of FOXO3 with SIRT1 results in the antioxidant response. Deacetylation of FOXO3 increases its ubiquitination and degradation in response to oxidative stress, thus facilitating the survival of endothelial precursor cells in oxidative stress [62].

The 3'-untranslated region of *KEAP1* directly binds with miR-141-3p, which thus increases apoptosis of vascular smooth muscle cells [63]. Inhibitor of nuclear factor κB (NF-κB) kinase subunit β (IKBKB) activates NF-κB, which is a key regulator of the inflammatory response, and is capable of binding with KEAP1 contained in the KEAP1–CUL3–RBX1 complex. Their interaction leads to IKBKB degradation and decreases NF-κB activation, thus reducing the inflammatory response [64].

TGFB2 is involved in regulating EMT. Its interaction network includes miR-454-3p, which binds with *TGFB2* and thus decreases EMT [65]. The regulation of apoptosis is also noteworthy; the interaction of miR-193a-3p with *TGFB2* prevents ferroptosis [66]. Protein–protein interactions of TGF-β2 include mostly a network related to the regulation of fibrosis. In myofibroblasts, the neuronal regeneration-related protein (NREP) binds with TGF-β2 to inhibit expression of type 1 and type 3 collagens, thereby decreasing the intensity of fibrotic transformation [67]. In contrast, the connective tissue growth factor (CTGF) directly binds with TGF-β2 to promote its profibrotic activity [68]. The interaction of TGF-β2 with TGF-β receptor 2 (TGFBR2) activates EMT [69].

Thus, our in silico analysis showed that the lncRNAs and mRNAs selected for the study function as regulators of the TGF-β/SMAD3, Wnt, PI3K/AKT, and Keap1/Nrf2 signaling cascades, which are involved in important cell processes, such as the antioxidant response to oxidative stress, apoptosis, inflammation, fibrogenesis, EMT, and cell aging.

Relative Expression Levels of lncRNAs and mRNAs in COPD Patients

Relative expression levels of the lncRNAs (TP53TG1, LINC00342, H19, MALAT1, DNM3OS, and MEG3) and mRNAs (PTEN, TGFB2, FOXO3, and KEAP1) were studied in PBMCs of the COPD patients and healthy controls. The results are summarized in Table 4 and Fig. 1.

Table 6. Analysis of correlations between expression levels of the lncRNA and mRNA genes (Spearman's correlation coefficient *r* and significance level *P*)

Gene	*DNM3OS*	*H19*	*LINC00342*	*MALAT1*	*MEG3*	*TP53TG1*	*TGFB2*	*PTEN*	*FOXO3*
H19	**0.307275** **0.02996**								
LINC00342	–0.00812 0.955395	–0.02958 0.772508							
MALAT1	**–0.28443** **0.043083**	0.085894 0.393072	**0.513173** **3.3×10^{-9}**						
MEG3	**0.518963** **5.81×10^{-5}**	**0.348803** **0.001416**	0.159364 0.138051	0.174391 0.098274					
TP53TG1	**0.345597** **0.007881**	–0.00027 0.997961	0.143321 0.138938	–0.10556 0.261518	**0.240212** **0.019699**				
TGFB2	0.247449 0.086492	0.138947 0.234485	–0.05147 0.644021	–0.01982 0.856252	0.210362 0.068157	**0.242294** **0.019699**			
PTEN	–0.07192 0.63092	–0.07884 0.452538	0.158737 0.10411	**0.435793** **1.13×10^{-6}**	0.035683 0.748773	–0.10639 0.268627	0.096514 0.339459		
FOXO3	–0.0781 0.585927	–0.0428 0.666151	0.122231 0.191171	**0.259988** **0.003411**	0.061188 0.564501	–0.1748 0.060558	0.184983 0.061396	**0.520288** **7.21×10^{-11}**	
KEAP1	–0.15095 0.290352	0.159005 0.119796	–0.01331 0.888743	0.113786 0.215925	0.090052 0.406826	–0.05824 0.541892	**0.249805** **0.012193**	–0.01431 0.871115	**0.317967** **0.000115**

Here and in Table 7, significant results are in bold.

A significant (greater than sixfold) decrease in TP53TG1 lncRNA level was observed in the COPD patients (FCh = 0.1532, FR = –6.5244, $P = 0.0001$) (Table 4). Expression of the MALAT1 lncRNA significantly increased in the COPD patients (FCh = 6.983, $P = 0.0001$). The LINC00342 lncRNA level in the COPD patients was almost three times higher than in the healthy subjects (FCh = 2.874, $P = 0.0029$). Expression of the DNM3OS lncRNA was significantly lower in the COPD patients (FCh = 0.5176, FR = –1.9317, $P = 0.0076$). The *TGFB2* mRNA expression level in MNCs of the COPD patients was significantly lower than in the healthy controls (FCh = 0.3639, FR = –2.7476, $P = 0.0001$).

The expression levels of the H19 lncRNA and *PTEN* and *KEAP1* mRNAs in PBMCs of the COPD patients were comparable with the levels observed in the control group. The relative expression levels of the MEG3 lncRNA and *FOXO3* mRNA in the COPD patients were more than twice higher than in the controls, but the between-group differences were nonsignificant.

Thus, the TP53TG1, LINC00342, DNM3OS, and MALAT1 lncRNAs and the *TGFB2* mRNA were found to differ in expression between the COPD patients and control subjects; i.e., the RNAs can be identified as differentially expressed in PBMCs in COPD. The TP53TG1, LINC00342, and DNM3OS lncRNA expression levels were for the first time assessed in PBMCs of COPD patients.

Evaluation of Predictive Significance for lncRNA and mRNA Differential Expression in COPD

Early COPD is asymptomatic, but the respiratory function of the lung and VC decrease gradually. A primary diagnosis is established when emphysema-related changes are substantial in lung tissue and small airways are obstructed so that breathlessness increases, therapy is ineffective, and quality of life drops dramatically [1, 2]. COPD biomarkers are therefore important to identify in order to allow early diagnosis of COPD and predisposition to rapid disease progression. ROC analysis was performed to evaluate the prognostic significance of the expression levels of the TP53TG1, LINC00342, MALAT1, and DNM3OS lncRNAs and the *TGFB2* mRNA in COPD (Fig. 2). The relative expression level of the TP53TG1 lncRNA showed a moderate prognostic significance in differentiating COPD patients and control subjects (AUC = 0.8685, 95% CI 0.8062–0.9309, $P = 0.001$, optimal cut-off point 0.6312, sensitivity = 0.9041, specificity = 0.7097). A moderate prognostic significance in differentiating COPD patients and controls was similarly established in the ROC analysis for the levels of the *TGFB2* mRNA (AUC = 0.75735, 95% CI 0.6678–0.8466, $P = 0.001$,

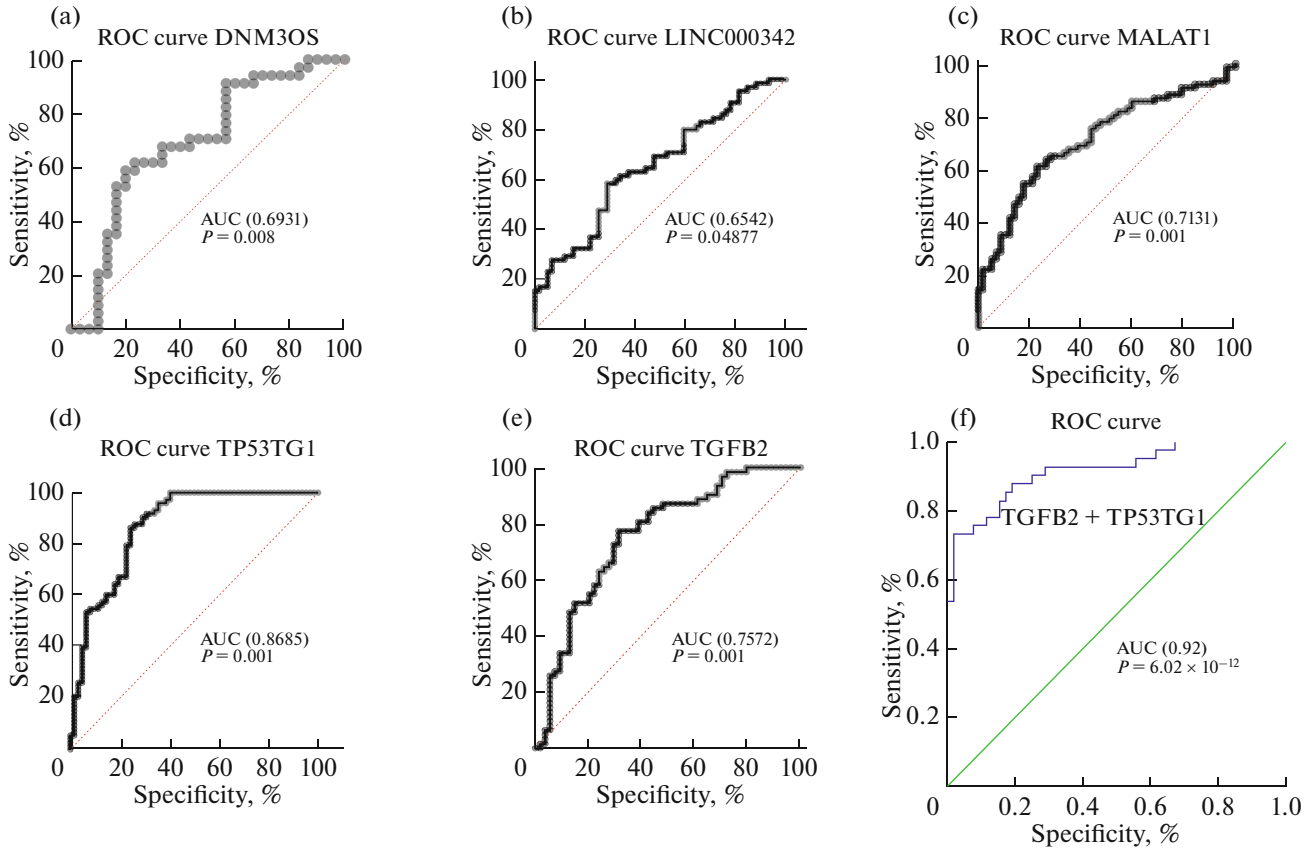

Fig. 2. ROC analysis of the prognostic significance of the lncRNAs and mRNAs regulated in PBMCs of the COPD patients: (a) DNM3OS lncRNA, (b) LINC000342 lncRNA, (c) MALAT1 lncRNA, (d) TP53TG1 lncRNA, and (e) *TGFB2* mRNA. AUC, area under the curve. (f) A prognostic model that includes simultaneous assessment of the TP53TG1 lncRNA and *TGFB2* mRNA expression levels.

optimal cut-off point 0.7923, sensitivity = 0.7742, specificity = 0.6850) and the lncRNAs MALAT1 (AUC = 0.7131, 95% CI 0.6261–0.8002, $P = 0.001$, optimal cut-off point 1.956, sensitivity = 0.6234, specificity = 0.7368), LINC00342 (AUC = 0.6542, 95% CI 0.5586–0.7498, $P = 0.0487$, optimal cut-off point 2.364, sensitivity = 0.6154, specificity = 0.661), and DNM3OS (AUC = 0.6931, 95% CI 0.5589–0.8274, $P = 0.008$, optimal cut-off point 0.7968, sensitivity = 0.6178, specificity = 0.7667).

A highly informative prognostic model of COPD development was based on multiple regression and ROC analyses and included simultaneous assessment of the expression levels of the TP53TG1 lncRNA and *TGFB2* mRNA in PBMCs (Table 5). The model has a high predictive potential (AUC = 0.92, 95% CI 0.86–0.98, sensitivity = 73.2%, specificity = 92.3%) (Fig. 2) and correctly distinguishes between COPD patients and subjects without COPD.

Based on the ROC analysis, the highest prognostic significance in discriminating COPD patients and healthy subjects is characteristic of the expression level of the TP53TG1 lncRNA and a combination of the expression levels of the TP53TG1 lncRNA and *TGFB2* mRNA.

Correlation Analysis

In view of the tight functional interactions between the lncRNAs and mRNAs under study, we assessed the correlations (Spearman's correlation coefficient r and significance level P) between their expression levels (Table 6). The DNM3OS relative expression level was found to correlate positively with the expression levels of H19 ($r = 0.307$, $P = 0.029$), MEG3 ($r = 0.518$, $P = 5.81 \times 10^{-5}$), and TP53TG1 ($r = 0.345$, $P = 0.0078$) and negatively with the expression level of MALAT1 ($r = -0.284$, $P = 0.043$). The MALAT1 expression level correlated positively with the levels of LINC00342 ($r = 0.513$, $P = 3.3 \times 10^{-9}$) and the *PTEN* ($r = 0.435$, $P = 1.13 \times 10^{-6}$) and *FOXO3* ($r = 0.259$, $P = 0.003$) mRNAs. The TP53TG1 lncRNA expression level correlated positively with the levels of MEG3 ($r = 0.240$, $P = 0.019$) and the *TGFB2* mRNA ($r = 0.242$, $P = 0.019$). A positive correlation was observed between the *TGFB2* and *KEAP1* expression levels ($r = 0.249$, $P = 0.012$) and between the *KEAP1* and *FOXO3*

Table 7. Correlations between expression levels of the genes under study and clinical parameters

Parameter	*DNM3OS*	*H19*	*LINC00342*	*MALAT1*	*MEG3*	*TP53TG1*	*TGFB2*	*PTEN*	*FOXO3*	*KEAP1*
Age	–0.1259 0.47809	–0.0918 0.50484	–0.2058 0.11459	**–0.313** **0.00742**	–0.1383 0.29615	0.12348 0.3085	**–0.3514** **0.00591**	–0.1809 0.14612	**–0.2951** **0.01249**	**–0.3382** **0.00513**
BMI	0.24633 0.16021	0.01465 0.91547	–0.1185 0.36724	**–0.3376** **0.00372**	–0.0428 0.74731	–0.0797 0.51201	–0.0358 0.78618	–0.1114 0.37305	–0.024 0.84223	0.10606 0.39299
Smoking index	–0.193 0.27418	0.04926 0.72095	–0.2233 0.08629	–0.1945 0.10155	0.07943 0.54981	0.15721 0.19368	–0.1431 0.27536	–0.0886 0.47908	–0.1508 0.2093	–0.1228 0.32233
FEV1/FVC, %	–0.0988 0.60347	–0.0678 0.65079	0.23456 0.09418	**0.27201** **0.03104**	0.15151 0.27411	0.0407 0.74753	**0.33801** **0.01161**	0.11216 0.39769	**0.42629** **0.00049**	**0.31171** **0.01447**
VC, %	0.21965 0.23513	–0.0207 0.88902	0.2071 0.13677	0.10873 0.39242	0.10165 0.46022	–0.0575 0.64638	0.06387 0.64315	–0.065 0.62178	0.07651 0.5479	–0.0651 0.61508
FVC, %	**0.42612** **0.03787**	0.018 0.92617	0.2617 0.12885	0.29973 0.06025	–0.0277 0.86683	–0.0713 0.64147	–0.1992 0.21788	0.03324 0.83445	0.1548 0.34021	–0.1454 0.37069
FEV1, %	0.13491 0.47722	–0.0456 0.76069	0.25271 0.07069	0.1913 0.13312	0.18177 0.18835	–0.0466 0.71266	0.20366 0.13587	0.10626 0.42313	**0.38502** **0.00183**	0.15945 0.21964

Spearman's correlation coefficient r and significance level P are shown.

expression levels ($r = 0.318$, $P = 0.0001$). A distinct positive correlation was detected between the expression levels of *FOXO3* and *PTEN* ($r = 0.52$, $P = 7.21 \times 10^{-11}$).

To estimate the contributions of the lncRNAs and mRNAs to the early development and progression of COPD, possible correlations with clinical and demographic parameters were analyzed (Table 7). The age was found to negatively correlate with the expression levels of MALAT1 ($r = -0.313$, $P = 0.007$), *TGFB2* ($r = -0.351$, $P = 0.006$), *FOXO3* ($r = -0.295$, $P = 0.012$), and *KEAP1* ($r = -0.338$, $P = 0.005$) in the COPD patients. Lung function parameters, which directly reflect the progression of airway obstruction and disease severity in COPD patients, were of particular interest to test for correlation with expression levels. FEV1/FVC was found to positively correlate with the expression levels of MALAT1 ($r = 0.272$, $P = 0.03$), *TGFB2* ($r = 0.338$, $P = 0.01$), *FOXO3* ($r = 0.426$, $P = 0.0004$), and *KEAP1* ($r = 0.311$, $P = 0.014$). FEV1 correlated with *FOXO3* expression ($r = 0.385$, $P = 0.0018$), and FVC correlated with DNM3OS expression ($r = 0.426$, $P = 0.037$).

The correlations with the lung function parameters indicate that the MALAT1 and DNM3OS lncRNAs and the *TGFB2, FOXO3*, and *KEAP1* mRNAs contribute to COPD development and are directly involved in lung tissue aging, which is associated with gradual reduction of airway conductance and the development of fibrosis- and emphysema-related changes.

DISCUSSION

High-level expression of the MALAT1 lncRNA in PBMCs was associated with COPD. The MALAT1 expression level correlated positively with the airway conductance (FEV1/FVC), which gradually decreases with COPD progression or natural aging of the lung. Higher MALAT1 expression levels in MNCs were more often observed in younger patients according to our correlation analysis, the finding being possibly related to an earlier COPD onset. The result is possibly explained by the involvement of the MALAT1 lncRNA in regulating the signaling cascades that are associated with cell senescence and inflammation. MALAT1 directly interacts with miR-200c via two highly complementary binding sites, as has been revealed by a bioinformatics analysis and confirmed by a luciferase reporter assay and real-time PCR [70]. It is known that miR-200c plays a crucial role in decreasing fibrosis-related transformation of lung epithelial cells [71]. The competitive interaction of MALAT1 with miR-200c may increase the fibrotic changes in lung epithelial cells, and such changes are of importance for emphysema development and lung tissue remodeling in COPD. MALAT1 additionally stimulates AKT/mTOR signaling by binding with a high-affinity sequence (a 7-nt binding site) of miR-206 and thus inhibiting miR-206 activity [49, 72]. This regulation may lead to bronchopulmonary dysplasia by increasing fibronectin 1 expression [73]. MALAT1 is capable of stimulating serine- and arginine-rich splicing factor 7 (SRSF7) and forkhead box P1 (FOXP1) by binding to a high-affinity site of miR-374b-5p [74]. The interactions increase EMT by modulating cell proliferation and apoptosis and controlling synthesis of matrix metalloproteinases and inflamma-

tory mediators in lung epithelial cells [75]. MALAT1 interacts with proteins of the FOX family via numerous microRNAs. For example, FOXA1 activity changes upon MALAT1 binding with miR-17-5p [76]. It is of special interest that MALAT1 decreases hypoxia-induced apoptosis in vascular cells by inhibiting miR-19b-3p [77]. Moreover, miR-19b-3p sequestration may increase expression of protein phosphatase 2 regulatory subunit B'ε (PPP2R5E) and BCL2-like 11 (BCL2L11), thereby similarly decreasing apoptosis in lung cancer cells [78]. MALAT1 can suppress miR-22-3p activity [79], thus facilitating inflammasome activation via a NLRP3-mediated mechanism, and increase STAT3-mediated inflammation of vascular cells [80]. MALAT1 can directly inhibit miR-590 by binding to its high-affinity site [81]. MALAT1 has been found to interact with high-affinity sites of miR-429 [82] and miR-23c [83]; the interactions may dysregulate angiogenesis and consequently lead to emphysema [50]. Inhibition of Toll-like receptor 4 (TLR4) by MALAT1 overexpression in acute lung injury inhibits NF-κB and MAP kinase p38. The effects can reduce the level of LPS-stimulated apoptosis and the production of inflammatory factors (IL-6 and TNF-α) [84]. The MALAT1 lncRNA is upregulated in lung tissue biopsy material of COPD patients and is involved in COPD pathogenesis [85]. Higher MALAT1 expression in the blood plasma correlates positively with the level of inflammatory cytokines and may provide a prognostic marker of COPD exacerbation risk [86]. COPD is considered to be a systemic inflammatory disease, and an increase in oxidative stress and a passage of lung inflammation into systemic circulation play an important role in its pathophysiology. COPD is characterized by simultaneous increases in macrophages in peripheral airways, lung parenchyma, and lung vessels and activated neutrophils, lymphocytes, and monocytes in circulation [87].

Thus, the results from our and other studies demonstrate that MALAT1 is upregulated in MNCs, lung tissue, and the serum in COPD patients, implicating MALAT1 in COPD development.

A positive correlation was observed between MALAT1 and LINC00342 relative expression levels. LINC00342 was also expressed to a significantly higher level in the COPD patients compared with the healthy subjects. LINC00342 activates the miR-15b/TPBG signaling cascade, thus promoting EMT in A549 lung carcinoma cells and leading to disease progression and metastasis in lung adenocarcinoma [42]. The role in various cancers has already been studied for LINC00342 [88]. LINC00342 binds with a 6-nt site in miR-15b with an energy high enough to ensure their stable interaction [42, 72]. Higher expression of LINC00342 in non-small cell lung cancer, its binding with a high-affinity site of miR-203a-3p [89], and inhibition of tumor suppression activities of p53 and PTEN are main factors responsible for higher proliferation and metastasis of cancer cells [17, 18]. The LINC00342 interaction partner miR-203a-3p functions as a regulator of the TGF-β/SMAD3 signaling pathway and facilitates TGF-β1-induced EMT in bronchial asthma [43].

We showed that expression of the TP53TG1 lncRNA is significantly lower in the COPD patients. The TP53TG1 level was found to positively correlate with the levels of DNM3OS and MEG3, and the bioinformatics analysis of the lncRNA–microRNA–mRNA interaction network supported the correlation. TP53TG1 is involved in regulating the TGF-β/SMAD3 signaling cascade to act as an antifibrotic factor and regulates lung cell apoptosis. TP53TG1 modulates the miR-18a-5p/PTEN axis in the A549 lung cancer cell line by binding with a high-affinity microRNA sequence, thus increasing the proapoptotic effect of cisplatin [40]. In a model of idiopathic lung fibrosis, TP53TG1 affects the ACTA2 (actin alpha 2, smooth muscle) and Fn1 (fibronectin 1) mRNAs, thus exerting antifibrotic activity toward fibroblasts [41]. There is evidence that TP53TG1 acts as a tumor suppressor. TP53TG1 triggers ubiquitin-dependent degradation of peroxiredoxin 4 (PRDX4) to block the WNT/β-catenin signaling pathway, thus inhibiting hepatocellular cancer progression and preventing liver fibrosis [14]. TP53TG1 has been shown to suppress breast cancer development by inhibiting the PI3K/AKT signaling pathway [90]. Thus, a high TP53TG1 level negatively affects the molecular mechanisms of accelerated cell aging by inhibiting the TGF-β/SMAD and PI3K/AKT signaling cascades. The role of TP53TG1 in COPD has not been studied earlier, and our findings obtained using PBMCs need verification using lung tissue samples.

A direct correlation between TP53TG1 lncRNA and *TGFB2* mRNA expression levels is of particular interest. Their combined testing showed the greatest prognostic significance in discriminating between COPD patients and healthy subjects according to our ROC analysis. The two transcripts are functionally associated because TP53TG1 acts as a regulator of the TGF-β/SMAD signaling cascade, in which TGF-β2 plays a key role. The *TGFB2* expression level in PBMCs was found to be lower in the COPD patients and to correlate with the patient age and lung function as assessed by FEV1/FVC. Based on bioinformatics analyses, TGF-β2 activates the TGF-β/SMAD2/SMAD3/SMAD4 signaling cascade to increase EMT, to facilitate fibrosis, and to exert an antiapoptotic effect [30]. In turn, SMAD2 and SMAD3 stimulate expression of the mesenchymal phenotype-associated genes *FN1*, *SNAI2*, and *MMP2* [91]. Higher activities of these genes may facilitate a remodeling of lung tissue and airways in COPD. On the other hand, TGF-β2 is involved in the antioxidant response. Its interaction with CCAAT enhancer-binding protein α (C/EBPα) positively affects differentiation and secretory activity of lung epithelial cells in the

case of hyperoxia-induced injury [92]. Large-scale RNA sequencing has shown that *TGFB2* expression in lung tissue is decreased in COPD patients [93].

Thus, changes in *TGFB2* expression profile in PBMCs of COPD patients may be associated with early disease onset and a rapid decrease in airway conductance.

The DNM3OS lncRNA expression level was found to be halved in the COPD patients and to correlate with FVC, which reflects a gradual progression of airway obstruction. The DNM3OS expression level correlated positively with the levels of the H19, MEG3, and TP53TG1 lncRNAs and negatively with the MALAT1 lncRNA level. Based on the bioinformatics analysis, DNM3OS interacts with the *MALAT1*, *H19*, *MEG3*, and *TP53TG1* genes through target mRNAs and microRNAs. DNM3OS is involved in regulating the TGF-β/SMAD cascade [20] and supporting the key processes of fibrotic transformation in upper airway cells, including their viability and migration potential. To exert these activities, DNM3OS inhibits miR-204-5p by interacting with a high-affinity 11-nt site and additional sequences [94] and thus activates huntingtin interacting protein 1 (HIP1) [95]. DNM3OS is fragmented to produce three microRNAs, which are each involved in regulating the key signaling cascades related to apoptosis, EMT, and cell proliferation [20]. It has been shown that miR-199a plays a role in regulating *SIRT1* expression in alveolar macrophages and thus modulates pulmonary inflammation in acute respiratory distress syndrome [96]. Dysregulation of DNM3OS and its derivative microRNAs is associated with various chronic diseases [19]. The DNM3OS expression level is elevated in pulmonary fibrosis [20]. Upregulation of miR-199a-5p alone in lung tissue has already been observed in COPD [97], while DNM3OS expression in COPD was for the first time studied in this work.

To summarize, we were the first to observe that expression of the DNM3OS lncRNA in PBMCs changes in COPD and that the changes correlate with breathing parameters. The correlation is possibly due to a role that DNM3OS and its derivative microRNAs play in regulating the TGF-β/SMAD signaling cascade and inflammation. The assumption needs further investigation with lung tissue samples.

No difference in expression between the COPD patients and healthy subjects was observed for the H19 and MEG3 lncRNAs and the *PTEN*, *FOXO3*, and *KEAP1* mRNAs. It should be noted that the correlation analysis implicated *FOXO3* and *KEAP1* in progression of airway obstruction. Namely, the expression levels of the two genes were found to correlate with parameters, suggesting their potential involvement in lung tissue aging, which is associated with a gradual decrease in airway conductivity, a remodeling of bronchi and bronchioles, and development of changes characteristic of fibrosis and emphysema.

To conclude, differential expression in COPD patients compared with healthy subjects was observed for the TP53TG1, LINC00342, DNM3OS, and MALAT1 lncRNAs and the *TGFB2* mRNA. TP53TG1, LINC00342, and DNM3OS were analyzed for the first time. Our findings need further verification in studies with lung tissue samples from COPD patients. A highly informative prognostic model was constructed for COPD development and included simultaneous assessment of the expression levels of the TP53TG1 lncRNA and *TGFB2* mRNA. The differentially expressed lncRNAs (TP53TG1, LINC00342, DNM3OS, and MALAT1) and the *TGFB2* protein-coding genes function to regulate apoptosis, inflammation, fibrogenesis, and EMT. The fact indicates that cell aging processes play an important role in the molecular pathogenesis of COPD. Our data may provide a basis for improving the diagnostic criteria and developing essentially new drugs.

ABBREVIATIONS AND NOTATION

COPD	chronic obstructive pulmonary disease
EMT	epithelial-to-mesenchymal transition
IPF	idiopathic pulmonary fibrosis
lncRNA	long noncoding RNA
MNC	mononuclear cell
VC	vital capacity
FVC	forced vital capacity
FEV1	forced expiratory volume in the first second

SUPPLEMENTARY INFORMATION

The online version contains supplementary material available at https://doi.org/10.1134/S0026893324700481.

Figures S1 and S2.

FUNDING

This work was supported by the Russian Science Foundation (project no. 23-25-00019, https://rscf.ru/project/23-25-00019/).

ETHICS APPROVAL AND CONSENT TO PARTICIPATE

All studies were conducted in accordance with good clinical practice regulations and the principles of biomedical ethics as outlined in the 1964 Declaration of Helsinki and its later amendments. They were also approved by the Ethics Committee of the Institute of Biochemistry and Genetics—Subdivision of the Ufa Federal Research Centre of the Russian Academy of Sciences, protocol no. 19 dated November 1, 2022.

Each participant in the study provided a voluntary written informed consent for providing biological material after

receiving an explanation of the potential risks and benefits, as well as the nature of the upcoming study.

CONFLICT OF INTEREST

The authors of this work declare that they have no conflicts of interest.

REFERENCES

1. Chuchalin A.G., Avdeev S.N., Aisanov Z.R., Belevskiy A.S., Leshchenko I.V., Ovcharenko S.I., Shmelev E.I. 2022. Federal guidelines on diagnosis and treatment of chronic obstructive pulmonary disease. *Pulmonologiya*. **32** (3), 356–392.
2. Agustí A., Celli B.R., Criner G.J., Halpin D., Anzueto A., Barnes P., Bourbeau J., Han M.K., Martinez F.J., Montes de Oca M., Mortimer K., Papi A., Pavord I., Roche N., Salvi S., Sin D.D., Singh D., Stockley R., López Varela M.V., Wedzicha J.A., Vogelmeier C.F. 2023. Global initiative for chronic obstructive lung disease 2023 report: GOLD executive summary. *Eur. Respir. J.* **61** (4), 2300239.
3. Ragland M.F., Benway C.J., Lutz S.M., Bowler R.P., Hecker J., Hokanson J.E., Crapo J.D., Castaldi P.J., DeMeo D.L., Hersh C.P., Hobbs B.D., Lange C., Beaty T.H., Cho M.H., Silverman E.K. 2019. Genetic advances in chronic obstructive pulmonary disease. insights from COPDGene. *Am. J. Respir. Crit. Care Med*. **200** (6), 677–690.
4. Choudhury G., MacNee W. 2017. Role of inflammation and oxidative stress in the pathology of ageing in COPD: Potential therapeutic interventions. *COPD*. **14** (1), 122–135.
5. Aghali A., Koloko Ngassie M.L., Pabelick C.M., Prakash Y.S. 2022. Cellular senescence in aging lungs and diseases. *Cells*. **11** (11), 1781.
6. Birch J., Anderson R.K., Correia-Melo C., Jurk D., Hewitt G., Marques F.M., Green N.J., Moisey E., Birrell M.A., Belvisi M.G., Black F., Taylor J.J., Fisher A.J, De Soyza A., Passos J.F. 2015. DNA damage response at telomeres contributes to lung aging and chronic obstructive pulmonary disease. *Am. J. Physiol. Lung Cell. Mol. Physiol*. **309** (10), L1124–1137.
7. Barnes P.J., Baker J., Donnelly L.E. 2019. Cellular senescence as a mechanism and target in chronic lung diseases. *Am. J. Respir. Crit. Care Med*. **200** (5), 556–564.
8. Brandsma C.A., de Vries M., Costa R., Woldhuis R.R., Königshoff M., Timens W. 2017. Lung ageing and COPD: Is there a role for ageing in abnormal tissue repair? *Eur. Respir. Rev*. **26** (146), 170073.
9. Puvvula P.K. 2019. LncRNAs regulatory networks in cellular senescence. *Int. J. Mol. Sci*. **20** (11), 2615.
10. Long Y., Wang X., Youmans D.T., Cech T.R. 2017. How do lncRNAs regulate transcription? *Sci. Adv*. **3** (9), eaao2110.
11. Ferrè F., Colantoni A., Helmer-Citterich M. 2016. Revealing protein-lncRNA interaction. *Brief Bioinform*. **17** (1), 106–116.
12. Markelov V.A., Korytina G.F., Aznabaeva Yu.G., Zulkarneev Sh.R., Akhmadishina L.Z., Zagidullin N.Sh. 2023. Contribution of signaling pathways associated with cellular senescence and regulatory non-coding RNAs to chronic obstructive pulmonary disease. *Genes & Cells*. **18** (2), 93–108
13. Lu Q., Guo Q., Xin M., Lim C., Gamero A.M., Gerhard G.S., Yang L. 2021. LncRNA TP53TG1 promotes the growth and migration of hepatocellular carcinoma cells via activation of ERK signaling. *Noncoding RNA*. **7** (3), 52.
14. Chen B., Lan J., Xiao Y., Liu P., Guo D., Gu Y., Song Y., Zhong Q., Ma D., Lei P., Liu Q. 2021. Long noncoding RNA TP53TG1 suppresses the growth and metastasis of hepatocellular carcinoma by regulating the PRDX4/β-catenin pathway. *Cancer Lett*. **513**, 75–89.
15. Ersahin T., Tuncbag N., Cetin-Atalay R. 2015. The PI3K/AKT/mTOR interactive pathway. *Mol. Biosyst.* **11** (7), 1946–1954. PMID: 25924008. https://doi.org/10.1039/c5mb00101c
16. Wang L., Chen Z., An L., Wang Y., Zhang Z., Guo Y., Liu C. 2016. Analysis of long non-coding RNA expression profiles in non-small cell lung cancer. *Cell. Physiol. Biochem*. **38** (6), 2389–2400.
17. Chen Q.F., Kong J.L., Zou S.C., Gao H., Wang F., Qin S.M., Wang W. 2019. LncRNA LINC00342 regulated cell growth and metastasis in non-small cell lung cancer via targeting miR-203a-3p. *Eur. Rev. Med. Pharmacol. Sci*. **23** (17), 7408–7418.
18. Tang H., Zhao L., Li M., Li T., Hao Y. 2019. Investigation of LINC00342 as a poor prognostic biomarker for human patients with non-small cell lung cancer. *J. Cell. Biochem*. **120** (4), 5055–5061.
19. Fellah S., Larrue R. Truchi M., Vassaux G., Mari B., Cauffiez C., Pottier N. 2023. Pervasive role of the long noncoding RNA DNM3OS in development and diseases. *Wiley Interdiscip. Rev. RNA*. **14** (2), e1736.
20. Savary G., Dewaeles E., Diazzi S., Buscot M., Nottet N., Fassy J., Courcot E., Henaoui I.S., Lemaire J., Martis N., Van der Hauwaert C., Pons N., Magnone V., Leroy S., Hofman V., Plantier L., Lebrigand K., Paquet A., Lino Cardenas C.L., Vassaux G., Hofman P., Günther A., Crestani B., Wallaert B., Rezzonico R., Brousseau T., Glowacki F., Bellusci S., Perrais M., Broly F., Barbry P., Marquette C.H., Cauffiez C., Mari B., Pottier N. 2019. The long noncoding RNA DNM3OS Is a reservoir of fibromiRs with major functions in lung fibroblast response to TGF-β and pulmonary fibrosis. *Am. J. Respir. Crit. Care Med.* **200** (2), 184–198.
21. Zeng R., Zhang R., Song X., Ni L, Lai Z., Liu C., Ye W. 2018. The long non-coding RNA MALAT1 activates Nrf2 signaling to protect human umbilical vein endothelial cells from hydrogen peroxide. *Biochem. Biophys. Res. Commun*. **495** (4), 2532–2538.
22. Ghafouri-Fard S., Esmaeili M., Taheri M. 2020. H19 lncRNA: Roles in tumorigenesis. *Biomed. Pharmacother*. **123**, 109774.
23. Lu Q., Guo Z., Xie W., Jin W., Zhu D., Chen S., Ren T. 2018. The lncRNA H19 mediates pulmonary fibrosis by regulating the miR-196a/COL1A1 axis. *Inflammation*. **41** (3), 896–903.

24. Xu J.L., Hua T., Ding J., Fan Y., Liu Z.J., Lian J.W. 2019. FOXF2 aggravates the progression of non-small cell lung cancer through targeting lncRNA H19 to down regulate PTEN. *Eur. Rev. Med. Pharmacol. Sci.* **23** (24), 10796–10802.

25. Al-Rugeebah A., Alanazi M., Parine N.R. 2019. MEG3: An oncogenic long non-coding RNA in different cancers. *Pathol. Oncol. Res.* **25** (3), 859–874.

26. Zhan H., Sun X., Wang X., Gao Q., Yang M., Liu H., Zheng J., Gong X., Feng S., Chang X., Sun Y. 2021. LncRNA MEG3 involved in NiO NPs-induced pulmonary fibrosis via regulating TGF-β1-mediated PI3K/AKT pathway. *Toxicol. Sci.* **182** (1), 120–131.

27. Cai B., Yang L., Do Jung Y., Zhang Y., Liu X., Zhao P., Li J. 2022. PTEN: An emerging potential target for therapeutic intervention in respiratory diseases. 2022. *Oxid. Med. Cell. Longev.* 4512503.

28. Chen C.Y., Chen J., He L., Stiles B.L. 2018. PTEN: Tumor suppressor and metabolic regulator. *Front. Endocrinol.* **9**, 338.

29. Ishtiaq Ahmed A.S., Bose G.C., Huang L., Azhar M. 2014. Generation of mice carrying a knockout-first and conditional-ready allele of transforming growth factor beta2 gene. *Genesis.* **52** (9), 817–826.

30. Schepers D., Tortora G., Morisaki H., MacCarrick G., Lindsay M., Liang D., Mehta S.G., Hague J., Verhagen J., van de Laar I., Wessels M., Detisch Y., van Haelst M., Baas A., Lichtenbelt K., Braun K., van der Linde D., Roos-Hesselink J., McGillivray G., Meester J., Maystadt I., Coucke P., El-Khoury E., Parkash S., Diness B., Risom L., Scurr I., Hilhorst-Hofstee Y., Morisaki T., Richer J., Désir J., Kempers M., Rideout A.L., Horne G., Bennett C., Rahikkala E., Vandeweyer G., Alaerts M., Verstraeten A., Dietz H., Van Laer L., Loeys B. 2018. A mutation update on the LDS-associated genes TGFB2/3 and SMAD2/3. *Hum. Mutat.* **39** (5), 621–634.

31. Stefanetti R.J., Voisin S., Russell A., Lamon S. 2018. Recent advances in understanding the role of FOXO3. *F1000Res.* **7**, F1000 Fac. Rev–1372.

32. Bellezza I., Giambanco I., Minelli A., Donato R. 2018. Nrf2-Keap1 signaling in oxidative and reductive stress. *Biochim. Biophys. Acta, Mol. Cell. Res.* 1865 (5), 721–733.

33. Cheng L., Wang P., Tian R., Wang S., Guo Q., Luo M., Zhou W., Liu G., Jiang H., Jiang Q. 2019. LncRNA2Target v2.0: A comprehensive database for target genes of lncRNAs in human and mouse. *Nucleic Acids Res.* **47** (D1), D140–D144.

34. Livak K.J., Schmittgen T.D. 2001. Analysis of relative gene expression data using real-time quantitative PCR and the 2(Delta Delta C(T)) method. *Methods.* **25** (4), 402–408.

35. Lin W., Liu H., Tang Y., Wei Y., Wei W., Zhang L., Chen J. 2021. The development and controversy of competitive endogenous RNA hypothesis in non-coding genes. *Mol. Cell. Biochem.* **476** (1), 109–123.

36. Bosson A.D., Zamudio J.R., Sharp P.A. 2014. Endogenous miRNA and target concentrations determine susceptibility to potential ceRNA competition. *Mol. Cell.* **56** (3), 347–359.

37. Jens M., Rajewsky N. 2015. Competition between target sites of regulators shapes post-transcriptional gene regulation. *Nat. Rev. Genet.* **16** (2), 113–126.

38. Yuan Y., Liu B., Xie P., Zhang M. Q., Li Y., Xie Z., Wang X. 2015. Model-guided quantitative analysis of microRNA-mediated regulation on competing endogenous RNAs using a synthetic gene circuit. *Proc. Natl. Acad. Sci. U. S. A.* **112** (10), 3158–3163.

39. Ebert M.S., Neilson J.R., Sharp P.A. 2007. MicroRNA sponges: Competitive inhibitors of small RNAs in mammalian cells. *Nat. Methods.* **4** (9), 721–726.

40. Xiao H., Liu Y., Liang P., Wang B., Tan H., Zhang Y., Gao X., Gao J. 2018. TP53TG1 enhances cisplatin sensitivity of non-small cell lung cancer cells through regulating miR-18a/PTEN axis. *Cell Biosci.* **8**, 23.

41. Sun J., Guo Y., Chen T., Jin T., Ma L., Ai L., Guo J., Niu Z., Yang R., Wang Q., Yu X., Gao H., Zhang Y., Su W., Song X., Ji W., Zhang Q., Huang M., Fan X., Du Z., Liang H. 2022. Systematic analyses identify the anti-fibrotic role of lncRNA TP53TG1 in IPF. *Cell Death Dis.* **13** (6), 525.

42. Su H., Yu S., Sun F., Lin D., Liu P, Zhao L. 2022. LINC00342 induces metastasis of lung adenocarcinoma by targeting miR-15b/TPBG. *Acta Biochim. Pol.* **69** (2), 291–297.

43. Fan Q., Jian Y. 2020. MiR-203a-3p regulates TGF-β1-induced epithelial-mesenchymal transition (EMT) in asthma by regulating Smad3 pathway through SIX1. *Biosci Rep.* **40** (2), BSR20192645.

44. van Nijnatten J., Brandsma C.A., Steiling K., Hiemstra P.S., Timens W., van den Berge M., Faiz A. 2022. High miR203a-3p and miR-375 expression in the airways of smokers with and without COPD. *Sci. Rep.* **12** (1), 5610.

45. Yu H., Qi N., Zhou Q. 2021. LncRNA H19 inhibits proliferation and migration of airway smooth muscle cells induced by PDGF-BB through miR-21/PTEN/Akt Axis. *J. Asthma Allergy.* **14**, 71–80.

46. Gutschner T., Hämmerle M., Eissmann M., Hsu J., Kim Y., Hung G., Revenko A., Arun G., Stentrup M., Gross M., Zörnig M., MacLeod A.R., Spector D.L., Diederichs S. 2013. The noncoding RNA MALAT1 is a critical regulator of the metastasis phenotype of lung cancer cells. *Cancer Res.* **73** (3), 1180–1189.

47. Lu L., Luo F., Liu Y., Liu X., Shi L., Lu X., Liu Q. 2015. Posttranscriptional silencing of the lncRNA MALAT1 by miR-217 inhibits the epithelial-mesenchymal transition via enhancer of zeste homolog 2 in the malignant transformation of HBE cells induced by cigarette smoke extract. *Toxicol. Appl. Pharmacol.* **289** (2), 276–285.

48. Chen W., Zhao W., Zhang L., Wang L., Wang J., Wan Z., Hong Y., Yu L. 2017. MALAT1-miR-101-SOX9 feedback loop modulates the chemo-resistance of lung cancer cell to DDP via Wnt signaling pathway. *Oncotarget.* **8** (55), 94317–94329.

49. Tang Y., Xiao G., Chen Y., Deng Y. 2018. LncRNA MALAT1 promotes migration and invasion of non-small-cell lung cancer by targeting miR-206 and activating Akt/mTOR signaling. *Anticancer Drugs.* **29** (8), 725–735.

50. Green C.E., Clarke J., Bicknell R., Turner A.M. 2021. Pulmonary microRNA changes alter angiogenesis in chronic obstructive pulmonary disease and lung cancer. *Biomedicines.* **9** (7), 830.

51. Shen Y., Yang Y., Li Y. 2020. MiR-133a acts as a tumor suppressor in lung cancer progression by regulating the LASP1 and TGF-β/Smad3 signaling pathway. *Thorac. Cancer*. **11** (12), 3473–3481.

52. Gokey J.J., Snowball J., Sridharan A., Speth J.P., Black K.E., Hariri L.P., Perl A.T., Xu Y., Whitsett J.A. 2018. MEG3 is increased in idiopathic pulmonary fibrosis and regulates epithelial cell differentiation. *JCI Insight*. **3** (17), e122490.

53. Li W., Qiu X., Jiang H., Han Y., Wei D., Liu J. 2016. Downregulation of miR-181a protects mice from LPS-induced acute lung injury by targeting Bcl-2. *Biomed. Pharmacother.* **84**, 1375–1382.

54. Su Y., Silva J.D., Doherty D., Simpson D.A., Weiss D.J., Rolandsson-Enes S., McAuley D.F., O'Kane C.M., Brazil D.P., Krasnodembskaya A.D. 2023. Mesenchymal stromal cells-derived extracellular vesicles reprogramme macrophages in ARDS models through the miR-181a-5p-PTEN-pSTAT5-SOCS1 axis. *Thorax*. **78** (6), 617–630.

55. Ma J., Chen S., Liu Y., Han H., Gong M. Song Y. 2022. The role of exosomal miR-181b in the crosstalk between NSCLC cells and tumor-associated macrophages. *Genes Genomics*. **44** (10), 1243–1258.

56. Wu H., Ma H., Wang L., Zhang H., Lu L., Xiao T., Cheng C., Wang P., Yang Y., Wu M., Wang S., Zhang J., Liu Q. 2022. Regulation of lung epithelial cell senescence in smoking-induced COPD/emphysema by microR-125a-5p via Sp1 mediation of SIRT1/HIF-1a. *Int. J. Biol. Sci*. **18** (2), 661–674.

57. Zhao Y., Li A. 2021. miR-19b-3p relieves intervertebral disc degeneration through modulating PTEN/PI3K/Akt/mTOR signaling pathway. *Aging.* **13** (18), 22459–22473.

58. Li H., Zhang P., Sun X., Sun Y., Shi C., Liu H., Liu X. 2015. MicroRNA-181a regulates epithelial-mesenchymal transition by targeting PTEN in drug-resistant lung adenocarcinoma cells. *Int. J. Oncol*. **47** (4), 1379–1392.

59. Horita H., Wysoczynski C.L., Walker L.A., Moulton K.S., Li M., Ostriker A., Tucker R., McKinsey T.A., Churchill M.E., Nemenoff R.A., Weiser-Evans M.C. 2016. Nuclear PTEN functions as an essential regulator of SRF-dependent transcription to control smooth muscle differentiation. *Nat. Commun*. **7**, 10830.

60. Chen G., Yu L., Dong H., Liu Z., Sun Y. 2019. MiR-182 enhances radioresistance in non-small cell lung cancer cells by regulating FOXO3. *Clin. Exp. Pharmacol. Physiol*. **46** (2), 137–143.

61. Wang S., Sun Y., Yao L., Xing Y., Yang H. Ma Q. 2024. The role of microRNA-23a-3p in the progression of human aging process by targeting FOXO3a. *Mol. Biotechnol*. **66** (2), 277–287.

62. Wang Y.Q., Cao Q., Wang F., Huang L.Y., Sang T.T., Liu F., Chen S.Y. 2015. SIRT1 protects against oxidative stress-induced endothelial progenitor cells apoptosis by inhibiting FOXO3a via FOXO3a ubiquitination and degradation. *J. Cell. Physiol*. **230** (9), 2098–2107.

63. Zhang C., Kong X., Ma D. 2020. miR-141-3p inhibits vascular smooth muscle cell proliferation and migration via regulating Keap1/Nrf2/HO-1 pathway. *IUBMB Life*. **72** (10), 2167–2179.

64. Thu K.L., Pikor L.A., Chari R., Wilson I.M., Macaulay C.E., English J.C., Tsao M.S., Gazdar A.F., Lam S., Lam W.L., Lockwood W.W. 2011. Genetic disruption of KEAP1/CUL3 E3 ubiquitin ligase complex components is a key mechanism of NF-kappaB pathway activation in lung cancer. *J. Thorac. Oncol*. **6** (9), 1521–1529.

65. Liao H., Liang Y., Kang L., Xiao Y., Yu T., Wan R. 2021. miR-454-3p inhibits non-small cell lung cancer cell proliferation and metastasis by targeting TGFB2. *Oncol. Rep.* **45** (5), 67.

66. Zhong L., Yang H., Zhu B., Zhao X., Xie M., Cao M., Liu C., Zhao D., Lyu Y., Shang W., Wang B., Wu Y., Sun X., Qiu G., Fu W., Jiang H. 2022. The TBX1/miR-193a-3p/TGF-β2 axis mediates CHD by promoting ferroptosis. *Oxid. Med. Cell. Longev*. **2022**, 5130546.

67. Paliwal S., Shi J., Dhru U., Zhou Y., Schuger L. 2004. P311 binds to the latency associated protein and downregulates the expression of TGF-beta1 and TGF-beta2. *Biochem. Biophys. Res. Commun*. **315** (4), 1104–1109.

68. Khankan R., Oliver N., He S., Ryan S.J., Hinton D.R. 2011. Regulation of fibronectin-EDA through CTGF domain-specific interactions with TGFβ2 and its receptor TGFβRII. *Invest. Ophthalmol. Vis. Sci*. **52** (8), 5068–5078.

69. Yang B., Bai J., Shi R., Shao X., Yang Y., Jin Y., Che X., Zhang Y., Qu X., Liu Y., Li Z. 2020. TGFB2 serves as a link between epithelial-mesenchymal transition and tumor mutation burden in gastric cancer. *Int. Immunopharmacol*. **84**, 106532.

70. Li Q., Zhang C., Chen R., Xiong H., Qiu F., Liu S., Zhang M., Wang F., Wang Y., Zhou X., Xiao G., Wang X., Jiang Q. 2016. Disrupting MALAT1/miR-200c sponge decreases invasion and migration in endometrioid endometrial carcinoma. *Cancer Lett*. **383** (1), 28–40.

71. Yang S., Banerjee S., de Freitas A., Sanders Y.Y., Ding Q., Matalon S., Thannickal V.J., Abraham E., Liu G. 2011. Participation of miR-200 in pulmonary fibrosis. *Am. J. Pathol*. **180** (2), 484–493.

72. Lin W., Liu H., Tang Y., Wei Y., Wei W., Zhang L., Chen J. 2021. The development and controversy of competitive endogenous RNA hypothesis in non-coding genes. *Mol. Cell. Biochem*. **476** (1), 109–123.

73. Zhang X., Xu J., Wang J., Gortner L., Zhang S., Wei X., Song J., Zhang Y., Li Q., Feng Z. 2013. Reduction of microRNA-206 contributes to the development of bronchopulmonary dysplasia through up-regulation of fibronectin 1. *PLoS One*. **8** (9), e74750.

74. Song J., Su Z.Z., Shen Q.M. 2020. Long non-coding RNA MALAT1 regulates proliferation, apoptosis, migration and invasion via miR-374b-5p/SRSF7 axis in non-small cell lung cancer. *Eur. Rev. Med. Pharmacol. Sci.* **24** (4), 1853–1862.

75. Andreas A., Maloy A., Nyunoya T. Zhang Y., Chandra D. 2022. The *FoxP1* gene regulates lung function, production of matrix metalloproteinases and in-

flammatory mediators, and viability of lung epithelia. *Respir. Res.* **23** (1), 281.

76. Wei S., Wang K., Huang X., Tang W., Zhao Z., Zhao Z. 2019. Knockdown of the lncRNA MALAT1 alleviates lipopolysaccharide-induced A549 cell injury by targeting the miR-17-5p/FOXA1 axis. *Mol. Med. Rep.* **20** (2), 2021–2029.
77. Liu H., Shi C., Deng Y. 2020. MALAT1 affects hypoxia-induced vascular endothelial cell injury and autophagy by regulating miR-19b-3p/HIF-1α axis. *Mol. Cell. Biochem*. **466** (1–2), 25–34.
78. Baumgartner U., Berger F., Hashemi Gheinani A., Burgener S.S., Monastyrskaya K., Vassella E. 2018. MiR-19b enhances proliferation and apoptosis resistance via the EGFR signaling pathway by targeting PP2A and BIM in non-small cell lung cancer. *Mol. Cancer*. **17** (1), 44.
79. Zhang Z., Li M., Zhang Z. 2020. lncRNA MALAT1 modulates oxaliplatin resistance of gastric cancer via sponging miR-22-3p. *OncoTargets. Ther.* **13**, 1343–1354.
80. Yang K., Li W., Duan W., Jiang Y., Huang N., Li Y., Ren B., Sun J. 2019. Resveratrol attenuates pulmonary embolism associated cardiac injury by suppressing activation of the inflammasome via the MALAT1-miR-22-3p signaling pathway. *Int. J. Mol. Med*. **44** (6), 2311–2320.
81. Zhou Q., Run Q., Li C.Y., Xiong X.Y., Wu X.L. 2020. LncRNA MALAT1 promotes STAT3-mediated endothelial inflammation by counteracting the function of miR-590. *Cytogenet. Genome Res*. **160** (10), 565–578.
82. Shen F., Zheng H., Zhou L., Li W., Xu X. 2019. Overexpression of MALAT1 contributes to cervical cancer progression by acting as a sponge of miR-429. *J. Cell. Physiol*. **234** (7), 11219–11226.
83. Liu C., Zhuo H., Ye M.Y., Huang G.X., Fan M., Huang X.Z. 2020. LncRNA MALAT1 promoted high glucose-induced pyroptosis of renal tubular epithelial cell by sponging miR-30c targeting for NLRP3. *Kaohsiung J. Med. Sci*. **36** (9), 682–691.
84. Lai X., Zhong J., Zhang A., Zhang B., Zhu T., Liao R. 2022. Focus on long non-coding RNA MALAT1: Insights into acute and chronic lung diseases. *Front. Genet*. **13**, 1003964.
85. Hu T.J., Huang H.B., Shen H.B., Chen W., Yang Z.H. 2020. Role of long non-coding RNA MALAT1 in chronic obstructive pulmonary disease. *Exp. Ther. Med*. **20** (3), 2691–2697.
86. Liu S., Liu M., Dong L. 2020. The clinical value of lncRNA MALAT1 and its targets miR-125b, miR-133, miR-146a, and miR-203 for predicting disease progression in chronic obstructive pulmonary disease patients. *J. Clin. Lab. Anal*. **34** (9), e23410.
87. Barnes P.J. 2016. Inflammatory mechanisms in patients with chronic obstructive pulmonary disease. *J. Allergy Clin. Immunol*. **138** (1), 16–27.
88. Shen P., Qu L., Wang J., Ding Q., Zhou C., Xie R., Wang H., Ji G. 2021. LncRNA LINC00342 contributes to the growth and metastasis of colorectal cancer via targeting miR-19a-3p/NPEPL1 axis. *Cancer Cell Int*. **21** (1), 105.
89. Chen Q.F., Kong J.L., Zou S.C., Gao H., Wang F., Qin S.M., Wang W. 2019. LncRNA LINC00342 regulated cell growth and metastasis in non-small cell lung cancer via targeting miR-203a-3p. *Eur. Rev. Med. Pharmacol. Sci*. **23** (17), 7408–7418.
90. Shao M., Ma H., Wan X., Liu Y. 2020. Survival analysis for long noncoding RNAs identifies TP53TG1 as an antioncogenic target for the breast cancer. *J. Cell. Physiol*. **235** (10), 6574–6581.
91. Deng H., Schwartz M.A. 2022. High fluid shear stress inhibits cytokine-driven Smad2/3 activation in vascular endothelial cells. *J. Am. Heart Assoc*. **11** (14), e025337.
92. Zhu Y., Chen X., Mi L., Wang Q., Zhu H., Ju H., Lu H. 2020. Sumoylation of CCAAT-enhancer-binding protein α inhibits lung differentiation in bronchopulmonary dysplasia model rats. *J. Cell. Mol. Med*. **24** (12), 7067–7071.
93. Ghosh A.J., Hobbs B.D., Yun J.H., Saferali A., Moll M., Xu Z., Chase R.P., Morrow J., Ziniti J., Sciurba F., Barwick L., Limper A.H., Flaherty K., Criner G., Brown K.K., Wise R., Martinez F.J., McGoldrick D., Cho M.H., DeMeo D.L., Silverman E.K., Castaldi P.J, NHLBI Trans-Omics for Precision Medicine (TOPMed) Consortium, Hersh C.P. 2022. Lung tissue shows divergent gene expression between chronic obstructive pulmonary disease and idiopathic pulmonary fibrosis. *Respir. Res*. **23** (1), 97.
94. He L., He G. 2021. DNM3OS facilitates ovarian cancer progression by regulating miR-193a-3p/MAP3K3 axis. *Yonsei Med. J*. **62** (6), 535–544.
95. Fang X., Tang Z., Zhang H., Quan H. 2020. Long noncoding RNA DNM3OS/miR-204-5p/HIP1 axis modulates oral cancer cell viability and migration. *J. Oral. Pathol. Med*. **49** (9), 865–875.
96. Liu Y., Guan H., Zhang J.L., Zheng Z., Wang H.T., Tao K., Han S.C., Su L.L., Hu D. 2018. Acute downregulation of miR-199a attenuates sepsis-induced acute lung injury by targeting SIRT1. *Am. J. Physiol. Cell. Physiol*. **314** (4), C449–C455.
97. Mizuno S., Bogaard H.J., Gomez-Arroyo J., Alhussaini A., Kraskauskas D., Cool C.D., Voelkel N.F. 2012. MicroRNA-199a-5p is associated with hypoxia-inducible factor-1α expression in lungs from patients with COPD. *Chest*. **142** (3), 663–672.

Translated by T. Tkacheva